# Electrochemical planarization of interconnect metallization

A. C. West H. Deligianni P. C. Andricacos

Studies of the electropolishing of copper are reviewed. Recent work intended to demonstrate the electrochemical planarization of the overburden in electroplated copper interconnect metallization is emphasized. Furthermore, two common reaction mechanisms invoked to explain the mass-transfer limitation required to achieve electropolishing are outlined and discussed within the context of anodic leveling, which has been more recently called electrochemical planarization. Finally, scaling arguments are used to demonstrate practical considerations for tool development and to speculate about uncertainties in anodic leveling theories.

### Introduction

The electrodeposition of copper for on-chip interconnects is now well established, and several papers devoted to aspects of the technology appear in this issue. Significant research efforts have led to and will continue to lead to an understanding of this electrodeposition process at unprecedented detail. For example, while studying the impact of additives on copper electrodeposition at submicron widths, a new leveling mechanism was discovered [1, 2]. Despite the advances made in the fundamental understanding of copper interconnect electrodeposition, the commercial baths used remain remarkably similar to those employed in printed circuit board manufacturing. For example, the electrolyte remains an "acid-copper" bath [3] containing sulfuric acid, cupric sulfate, and organic additives that remain very similar in functionality to the original state of the art.

The present paper discusses the possible use of the electrochemical dissolution of copper for on-chip interconnect metallization. In contrast to the electrodeposition technologies, for which a baseline electrolyte and additive package that had already been implemented in industrial practice served as a starting point, it remains unknown whether already established electropolishing-bath compositions can be so easily adopted or whether more novel chemistries will be needed. Furthermore, the long-term technological importance of electrochemical dissolution has not

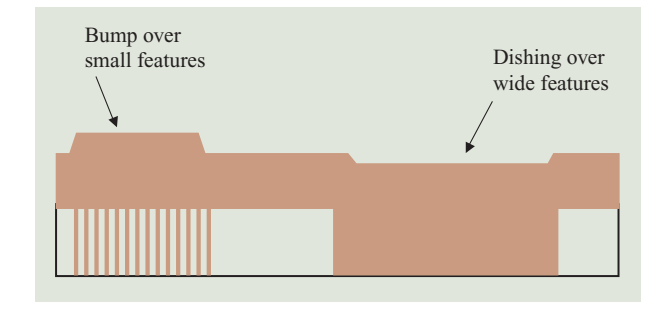
yet been established, partly because, while practical dissolution rates may be achieved, its planarization ability has not been unambiguously demonstrated on a sufficient variety of feature dimensions and patterns.

A practical need for electrochemical polishing arises because electrodeposition processes fill features with sizes that typically span at least an order of magnitude even within a single level of metallization. For this and other reasons, the overburden of the deposited film may be much larger than the smallest feature size, as shown in **Figure 1**. For example, even for the 100-nm node, it is common that more than one  $\mu$ m of copper must be electrodeposited, and the topography above the largest figures may exhibit dishing. This extra copper must be removed in a subsequent processing step. For this reason, alternative designs such as electrochemical mechanical deposition, in which mechanical removal is coupled with the electrodeposition process, reducing the overburden significantly, have been proposed [4].

At present, chemical mechanical planarization (CMP) is the primary method used for removing the overburden, and the removal rate is controlled in part by the mechanical force applied during the polishing step [5, 6]. CMP may also be employed in the same step to remove the liner material overlying the dielectric. Thus, electrochemical methods for the removal of liner films such as Ta or TaN may also be of interest. Nevertheless, the present paper focuses on copper.

©Copyright 2005 by International Business Machines Corporation. Copying in printed form for private use is permitted without payment of royalty provided that (1) each reproduction is done without alteration and (2) the Journal reference and IBM copyright notice are included on the first page. The title and abstract, but no other portions, of this paper may be copied or distributed royalty free without further permission by computer-based and other information-service systems. Permission to republish any other portion of this paper must be obtained from the Editor.

0018-8646/05/\$5.00 @ 2005 IBM



Schematic diagram illustrating that the overburden thickness of an electrodeposited film may be much larger than the smallest feature width. Commonly, the overburden is thicker than average above the smallest features, and dishing below the average overburden thickness is observed above the wide features. The bump over the small features and the dish size are strongly dependent on the electrochemical deposition process.

In the near future, the ability to achieve acceptable polishing rates with CMP may be compromised by the introduction of low-dielectric-constant materials [6, 7] that do not have the requisite mechanical properties to withstand large mechanical forces during CMP. Alternative metal-removal methods should enable high dissolution rates without subjecting the substrate to excessively large pressures. Electrochemical dissolution methods, either as a CMP replacement or a complement to CMP, have received a fair amount of recent attention [8–16].

Depending on bath temperature, electrolyte composition, applied voltage, and fluid flow, electrochemical removal rates may be anticipated to correspond to current densities between 10 and 100 mA/cm<sup>2</sup>. Assuming that the dissolution product is  $Cu^{2+}$  and that a 100% current efficiency is achieved, the etch rate u can be related to current density through an application of Faraday's law:

$$u = \frac{V_{\rm m}i}{2F},\tag{1}$$

where  $V_{\rm m}$  is the molar volume of copper, i is the current density, and F is Faraday's constant (96,487 coulombs per mole). A complete list of symbols is also provided at the end of the paper.

Since the molar volume of copper  $V_{\rm m}=7.1~{\rm cm}^3/{\rm mol}$ , current densities between 10 and 100 mA/cm<sup>2</sup> correspond to a metal-removal rate between 0.2 and 2  $\mu$ m/min. The need to operate at high current densities to achieve a desirable surface finish may in fact result in etch rates that are too large to enable precise process control. Thus, pulsed etching can be employed, as demonstrated by Datta and co-workers [17, 18]. At least at low pulse

frequencies, the duty cycle (the ratio of on-time to total etch time) can be used as a means of controlling the time-averaged etch rate, without the need to modify flow conditions or the applied potential to achieve the same surface finish.

# **Background**

Electropolishing processes operate at or above the current density at which the dissolution rate is controlled by the rate of mass transfer of a limiting reactant or product to or from the electrode surface. This rate is often called the limiting-current density and is a function of the viscosity of the electrolyte, the diffusion coefficient of the limiting reactant, and the forced or natural convection in the electropolishing tool.

Operation at the limiting-current density causes a surface peak to dissolve more rapidly than a valley because the peak is more accessible to the bulk solution. Furthermore, operation under conditions in which the mass transfer dictates the dissolution rate eliminates the propensity for the roughening of an initially smooth interface due to variations in etch rate of crystallographic faces [19, 20].

This situation can be contrasted with electrodeposition processes. First, variations in growth rate with the crystallographic face may lead to deposits with a preferred crystallographic orientation with improved electromigration resistance and thus may be desired [21, 22]. Second, the interface is unstable if the growth is controlled by mass transfer of cupric ions to the surface, leading to the formation of burnt deposits with poor adhesion, dendritic growth, or other unacceptable morphologies [23, 24]. For this reason, electrodeposition processes are often designed to operate at a small portion (e.g., 10–30%) of the limiting-current density.

Operation at the limiting current implies that *potential* control instead of the more typical *current* control employed in electrodeposition may be the desired means of operating an electropolishing tool. Furthermore, operation at the limiting-current density dictates that fluid flow will be a key tool-design consideration in developing an electrochemical planarization technology. Fluid flow almost certainly remains an important consideration for electrodeposition processes, especially because significant mass-transfer limitations can be expected as a result of the presence of organic additives. Nevertheless, the influence of fluid flow on the wafer-scale plating distribution can be expected to be less significant than for electropolishing.

Operation at the limiting-current density may lead to another key design consideration: Currents tend to be high, implying that wafer-contact resistances should be minimized and that the potential drops through the system, due to ohmic resistances in the electrolyte or in the substrate, may be very high. Large ohmic potential drops may lead to large spatial variations in the local potential difference between the electrolyte and electrode, which could have an impact on the possibility of maintaining the dissolution reaction at a rate controlled by mass transfer on all locations across the wafer. An estimate of a design tolerance can be obtained from the size of the limiting-current plateau on the polarization curve of the system.

**Figure 2** shows polarization curves for the dissolution of copper rotating disk electrodes into 85 wt.% phosphoric acid [25]. The limiting-current plateau extends for approximately 1.2 V. For a rotating disk electrode, the potential of the electrolyte as a function of radial position, assuming operation at the limiting current, may be found in the text by Newman [26]. The center-to-edge potential difference is given by

$$\Delta\phi_{\rm electrolyte} = \frac{0.363 r_0 i_{\rm avg}}{\kappa}. \tag{2}$$

For a copper disk with radius  $r_0 = 15$  cm in phosphoric acid with  $\kappa = 0.12~\Omega^{-1}$ -cm<sup>-1</sup>, the potential difference is 0.9 V when  $i_{\rm avg} = 20~{\rm mA/cm}^2$ .

Of course, a practical tool is not constructed as a rotating disk electrode. Rather, the tool is likely designed to eliminate wafer-edge effects associated with the electrical field. Thus, the electrolyte potential variation is significantly less; it can be estimated by solving Laplace's equation for the actual tool geometry, assuming a constant-current density at the wafer [26]. The tradeoff in designing the tool to eliminate electrical-field edge effects may be a compromise from the ideal flow of a rotating disk electrode that results in a uniform limiting-current distribution.

A more significant concern may be the potential variations in the substrate due to the terminal effect, especially for the final stages of the dissolution process, when the copper layer is thin [27, 28]. By assuming that the current density is constant across the wafer, the center-to-edge potential variation can be estimated from the expression [29]

$$\Delta\phi_{\text{substrate}} = \frac{r_0^2 i_{\text{avg}}}{4\sigma\lambda}.$$
 (3)

The terminal effect is typically not important during the initial stages of dissolution. For example, for a wafer with radius  $r_0=15$  cm with  $\sigma=5\times10^5~\Omega^{-1}$ -cm (corresponding to the conductivity of Cu) and  $\lambda=1.0~\mu\text{m}$ , the potential drop in the initial stages of dissolution is approximately 20 mV when  $i_{\text{avg}}=20~\text{mA/cm}^2$ . However, at the final stages of dissolution, the potential drop can be significant. For example, assuming that an insignificant amount of Cu remains and that a 30-nm Ta liner (with

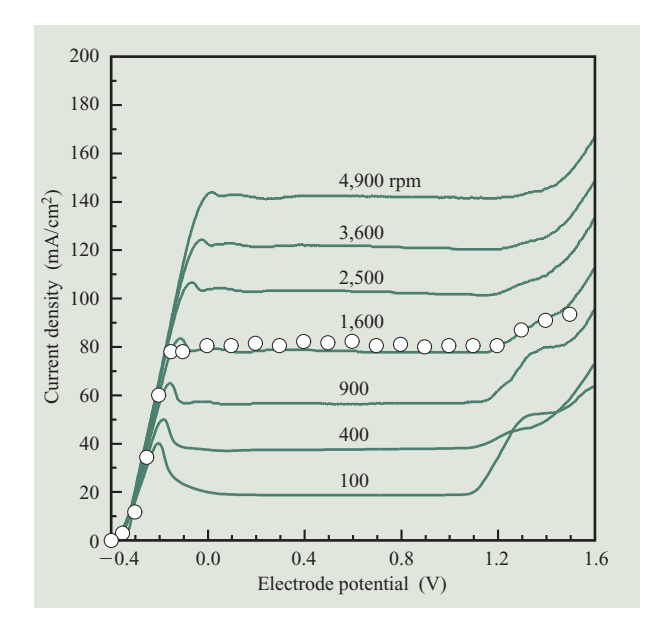


# Figure 2

Polarization curves for copper dissolution into 85-wt.% phosphoric acid at several rotation speeds. The solid curves were obtained at a sweep rate of 5 mV/s, and the data points represented by the open circles were obtained from steady-state current density measurements performed at 1,600 rpm. The limiting current plateau extends from roughly -0.2 V to 1.0 V at a rotation speed of 100 rpm. From [25], with permission.

 $\sigma = 3 \times 10^4 \ \Omega^{-1} \text{-cm}^{-1}$ ) carries most of the current, the potential drop can be estimated to be approximately 12 V. This is of course an overestimate, because the very existence of the large substrate resistance will cause the current distribution to be nonuniform. Nevertheless, it represents an estimate of the importance of the terminal effect.

Large spatial variations in the local potential difference between the electrolyte and electrode, whether they are caused by the ohmic resistance in the electrode or electrolyte, may render it impossible to maintain polishing conditions across the entire wafer, leading to nonuniformities in surface finish and metal-removal rate. Nonuniform removal rates may cause many technological problems, including the creation of electrically isolated metal islands of copper that cannot be electrochemically removed unless the conductivity of the liner is sufficient. Localized electropolishing tools that remove metal layers from the wafer center out to the edge have been proposed as one approach to circumventing wafer-scale nonuniformities [30].

### **Recent work**

Electropolishing and the electrochemical etching or machining of metals have been known for decades

40

[31–33]. Excellent reviews have been provided by Landolt [34, 35] and Datta [36]. The focus of this review is on recent work related to wafer-scale electropolishing as a means of planarization.

Contolini, Mayer, and co-workers were the first to demonstrate and to discuss the advantages of electropolishing as a replacement or complement of CMP [9–11]. They achieved a metal-removal rate between 0.25 and 1.0  $\mu$ m/min and very good uniformity with 100-mm and 175-mm samples. Furthermore, they demonstrated a significant reduction in the roughness of blanket copper films that had been previously electroplated to a rather large thickness of 8.0  $\mu$ m. They have demonstrated to a more limited degree planarization of 5.0- $\mu$ m features.

Two potential drawbacks to the electropolishing process were also demonstrated: 1) an incubation time before the onset of surface polishing and 2) residual islands of copper that are not completely removed, as discussed briefly in the previous section. They proposed that residual islands could be subsequently removed via another etch step or through CMP. The incubation time was asserted to be related to the time required to set up a mass-transfer-controlled dissolution rate and was approximately 1.5 minutes in their system.

Assuming the formation of a diffusion layer close to the electrode surface of thickness  $\delta$ , the time required to achieve a mass-transfer limitation can be estimated as  $\delta^2/D$ , where D is the diffusion coefficient of the limiting species. Given that D is likely between  $10^{-7}$  and 10<sup>-8</sup> cm<sup>2</sup>/s for a phosphoric-acid electrolyte at room temperature, and  $\delta$  may be expected to be a relatively large value of 10  $\mu$ m in part because of the high kinematic viscosity of phosphoric acid, their conjecture that the incubation time is related to the time required to set up mass-transfer limitations appears reasonable. If the amount of copper that is to be removed is very thick, this incubation time may not be problematic. However, the incubation period is more serious when the copper overburden is reduced in thickness. Interestingly, while a large viscosity is often cited as important for establishing good electropolishing conditions because it leads to a large  $\delta$ , the large viscosity may also lead to a large incubation time, a potentially major drawback for onchip planarization.

Padhi et al. [12] have discussed the importance of the incubation time more explicitly. They used an experimental polishing tool for 200-mm-diameter wafers with concentrated phosphoric acid as the electrolyte and employed galvanostatic control rather than the more conventional potentiostatic control to demonstrate how the anode potential varies with time as a function of the wafer rotation speed. An abrupt jump in the potential corresponds to the onset of mass-transfer-controlled dissolution, and correspondingly electropolishing.

Furthermore, they demonstrated that this incubation time should be proportional to the square of the applied current, implying that less copper material has to be removed at high applied currents before polishing commences. However, operation at a high applied current leads to oxygen evolution at times greater than the incubation time. The resulting oxygen bubbles, some of which adhere to the anode surface, lead to nonuniform etching. Contolini, Mayer, and co-workers also report a detrimental impact of oxygen bubbles on surface finish [9–11].

The compromise between reducing the incubation time and avoiding oxygen evolution led to an optimum current. Similarly, the flow conditions had to be optimized. Under the optimized conditions, some planarization of features was achieved. Wafer-scale uniformity was good except near the edges, where the metal-removal rate was significantly higher. The authors attributed this variation to the terminal effect, as discussed in the previous section.

Chang et al. [13–15] have contributed three interesting papers related to the mechanisms of electropolishing, the use of additives to improve planarization, and pattern effects. In the first paper [13], the authors focus on the reaction mechanism and on the dishing of features in relation to that which is attainable in CMP, and they assert that electrochemical planarization methods can readily be integrated with other planarization methods. The authors claim from electrochemical impedance spectroscopy measurements and from X-ray photoelectron spectroscopy that the measured limiting-current density is related to the formation of a passivation layer during dissolution. This conclusion seems contrary to many of the other references outlined in the next section

In a second paper [14], the authors have demonstrated that the phosphoric acid electrolyte can be modified to improve the planarization of features. The effects of various additives were examined, and it was concluded that the addition of small concentrations of polyethylene glycol (PEG) or citric acid can enhance process performance. The PEG appears to suppress oxygen evolution, presumably leading to a reduction or elimination of bubble-induced defects. The citric acid is known to complex copper ions, and it is speculated by the authors that a gradient in citric acid within the feature helps to establish a greater difference in dissolution rate between the feature bottom and the outer surface than is obtained in phosphoric acid alone.

In the third paper [15], the authors have provided perhaps the most complete published study of feature planarization. They have shown that the degree of planarization achieved for a given amount of material removed is a function of feature size as well as pattern density. The smaller, high-aspect-ratio features can be more rapidly planarized than large, low-aspect-ratio features. Such results are consistent with mass-transfer considerations. The space between features (i.e., the pattern pitch) was found to be less important, but for a given feature width, the degree of planarization was found to decrease with increasing spacing.

Huo et al. [16] have recently published an interesting study of electrochemical planarization using four phosphoric-acid-based electrolytes and a 70-wt.% hydroxyethylidenediphosphoric acid (HEDP) electrolyte. They studied electropolishing mechanisms using electrochemical impedance spectroscopy and concluded that in the phosphoric acid electrolyte an acceptor mechanism, discussed in the next section, is probably the best explanation for the limiting-current plateau, in contradiction of the assertions of Chang et al. They concluded that a salt-film mechanism prevails for the HEDP electrolyte. Furthermore, they demonstrated a rather dramatic improvement in planarity when HEDP is employed instead of phosphoric acid.

In a related study, Huo et al. [8] measured the polarization behavior of copper oxidation in HEDP/ phosphoric-acid mixtures. The resulting surface finish of blanket copper films, as measured by atomic force microscopy, was reported. The influence of the HEDP/ phosphoric-acid ratio on the limiting current density, which is translatable into a practical metal-removal rate, and on the decline in surface roughness was reported. On the basis of these results, an optimal composition was reported.

In the next two sections, we continue the review of the literature, with an emphasis on summarizing concepts that may facilitate the development of an electropolishing process. Furthermore, we attempt to speculate on some theoretical considerations that may play a role in electrolyte development.

# **Mechanisms**

As already indicated, Figure 2 shows several polarization curves for the dissolution of copper rotating disk electrodes into 85-wt.% phosphoric acid [25]. Each curve corresponds to a different electrode rotation speed and is characterized by a well-defined limiting-current plateau. The small current peaks prior to the limiting-current plateau result from using a potential sweep rate of 5 mV/s. The magnitude of the peak decreases with decreasing sweep rate. In contrast to the Cu/phosphoric-acid system, other systems, in which a salt film precipitates on the electrode, often display an undershoot in current density immediately following the peak. The limiting-current plateau can be confirmed to be the result of mass-transfer limitations in the electrolyte by verifying that the limiting-current density  $i_{\rm lim}$  is proportional to the

square root of rotation speed [37–39]. In contrast, aluminum dissolution in phosphoric acid exhibits a limiting-current plateau for a range of temperatures, but only at high temperatures is the process limited by mass transfer in the electrolyte [40]. Correspondingly, a smooth surface finish is attained only at the higher temperatures.

Finally, it should also be noted that mass-transfercontrolled dissolution does not ensure a smooth finish. For example, when copper is dissolved in a concentrated cupric sulfate electrolyte, a limiting-current plateau that varies linearly with the square root of rotation speed results. However, the surface is dull, with a coarse microtexture [41].

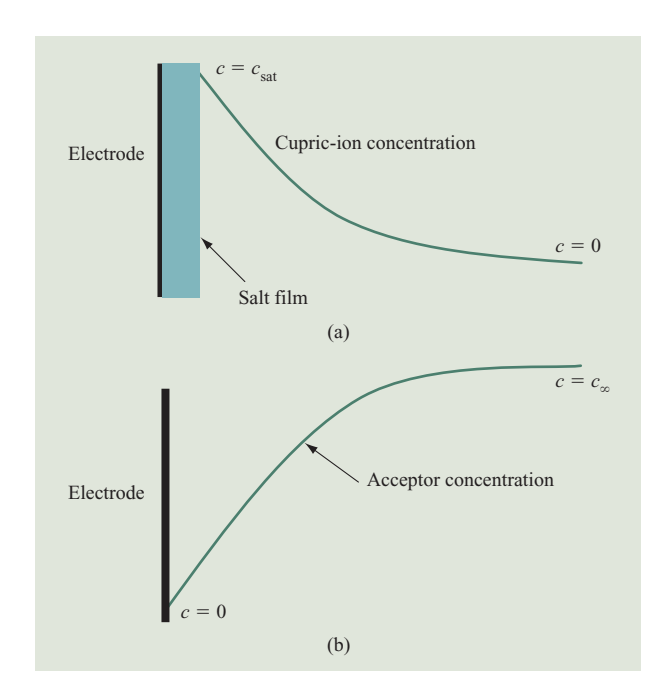
With reference to Figure 2, operation below the limiting-current plateau (<-0.2 V for a rotation speed of 400 rpm) results in a dull surface finish, exhibiting preferential crystallographic attack. On the limiting-current plateau, the resulting surface finish is mirrorlike. Above the limiting current, the surface remains mirrorlike, but (at least in some cases) with randomly distributed pits, presumably arising because of the presence of oxygen bubbles that adhere to the copper surface. The oxygen bubbles result from the onset of a second reaction at roughly 1.2 V (for a rotation speed of 100 rpm):

$$2H_2O \rightarrow O_2 + 4H^+ + 4e^-.$$
 (4)

Since the solubility of oxygen in water is low, bubbles are rapidly formed once water oxidation occurs. For this reason, Chang et al. [14] evaluated the influence of PEG on the polarization curve for copper dissolution into concentrated phosphoric acid. They reported a significant decrease in the rate of reaction 4, although they did not report a shift in the onset potential, implying that reaction 4 could not be completely suppressed. It was not clear that the lowered reaction rate is sufficient to eliminate bubbles completely because of the very low solubility of oxygen in most electrolytes; however, they did report an improvement in surface finish.

As outlined in the Introduction, there is a theoretical rationale for the correlation between smooth surface finish and operation at the limiting-current density. However, the cause of the mass-transfer limitations is not obvious, as discussed in this section. Salt-film and acceptor mechanisms have been invoked to explain the plateau, and are depicted in **Figure 3**. The relevance of the two alternative mechanisms depends on the combination of electrode material and electrolyte that is under investigation.

In a salt-film mechanism, metallic product ions accumulate near the electrode surface until the solubility of a salt is exceeded. Once the solubility is exceeded or once the solution becomes sufficiently supersaturated to



Schematic diagrams illustrating (a) a salt-film mechanism, in which the process is limited by transport of reaction product away from the electrode surface, and (b) an acceptor mechanism, in which the dissolution process is limited by transport of an "acceptor" to the electrode surface.

allow for nucleation of the new phase, a solid salt film precipitates on the electrode surface. In the presence of the film, the local concentration of the cationic and anionic components of the salt are determined by their solubility product, and the dissolution rate is subsequently dictated by mass transfer of the metallic ions from the film/electrolyte interface to the bulk solution.

In an acceptor mechanism, it is hypothesized that the metallic ions must be complexed (for example, by water molecules in aqueous electrolytes) before they can be transported from the electrode surface. In an acceptor theory, the dissolution process is limited by transport of the complexing or acceptor agent to the electrode surface.

Experimental studies that attempt to distinguish between the two mechanisms may seem straightforward. However, simple studies that modify bath composition, for example, as a means of identifying the mechanisms are often inconclusive, especially for an acceptor mechanism. Temperature is another variable that can be exploited in discriminating between mechanisms, although the resulting variations in physical properties also make difficult an unambiguous interpretation.

Ex situ surface-characterization studies have also tended to be inconclusive, since any salt film quickly dissolves once metal oxidation ceases. *In situ* studies to check for the formation of a solid film on the electrode surface (evidence for a salt-film mechanism) during electropolishing, either via optical methods or electrochemical measurements, appear to have had more success in distinguishing between mechanisms [42, 43].

### Salt-film mechanism

Salt-film mechanisms have probably received more widespread acceptance because they may be easier to prove via experiment and because they may be more intuitive because of their relevance to some aspects of localized corrosion and passivation [44].

Iron dissolution into chloride-containing electrolytes such as NaCl is an example for which the experimental evidence indicates clearly that a salt-film mechanism is applicable [45]. At or below the limiting-current plateau, ferrous ions are the predominant oxidation product, viz.,

$$Fe \to Fe^{2+}(aq) + 2e^{-},$$
 (5)

as can be determined by weight-loss measurements [43]. Even for copper dissolution, in which cupric ions are likely to be the primary dissolution product, such weight-loss measurements are useful in determining the current efficiency, a measure of the importance of side reactions such as reaction 4 [25].

During iron electropolishing, the ferrous ions at the electrode surface increase until the solubility product for FeCl<sub>2</sub> is exceeded. The salt-precipitation reaction then occurs:

$$Fe^{2+}(aq) + 2Cl^{-}(aq) = FeCl_{2}(s).$$
 (6)

The salt film is believed to be in local equilibrium with the ferrous and chloride ions, effectively setting the surface concentration of ferrous ions:

$$K_{\rm sp} = c_{\rm Cl}^2 c_{\rm Fe}.\tag{7}$$

At room temperature,  $K_{\rm sp} = 77 \text{ M}^3$  [46]. For a binary electrolyte, this solubility product corresponds to a concentration of ferrous chloride of 4.3 M.

Once the ferrous-ion concentration is set by the equilibrium constraint of the salt film, the limiting-current density on a rotating disk electrode can be expressed approximately as

$$i_{\text{lim}} = 0.62 n F \Omega^{1/2} (D_{\text{Fe}}^{2/3} v^{-1/6} \Delta c),$$
 (8)

where  $\Delta c$  is the concentration difference between the surface and the bulk solutions.

$$\Delta c = (c_{\text{Fe.sat}} - c_{\text{Fe.}\infty}),\tag{9}$$

and n, the number of electrons transferred, is 2 in this example. The bulk concentration  $c_{{\rm Fe},\infty}=0$  for an NaCl

electrolyte, and the saturation concentration of ferrous ions depends on the local concentration of chloride ions at the salt interface. As a first approximation, one may assume that the chloride concentration at the film/ electrolyte interface is equal to its bulk concentration.

While Equation (8) is a good approximation, electrical migration (the movement in the electrolyte of a charged species in response to an electrical field) may be anticipated to modify the limiting current [47] because, at least near the surface, the ferrous-ion concentration is comparable to or larger than the bulk concentration of Na<sup>+</sup>, implying that the ferrous-ion transference number is non-negligible. Furthermore, the chloride-ion concentration at the surface will be higher than in the bulk to counteract the electrical-migration-induced flux of chloride ions to the solution. Thus, a comparison of experiment with Equation (8) may not be in quantitative agreement, even if all of the physical properties are known with precision.

Nevertheless, the addition of a salt to the electrolyte would seem to be a relatively straightforward method of testing for a salt-film mechanism. Thus, according to Equations (8) and (9), the replacement of the NaCl with a 4.0-M FeCl $_2$  electrolyte should lead to roughly an order of magnitude decrease in limiting-current density. This indeed occurs, helping to validate the salt-film hypothesis. However, quantitative comparisons are difficult because the addition of such a large quantity of salt affects the electrolyte transport properties, e.g.,  $D_{\rm Fe}$  and the kinematic viscosity, as well as the influence of electrical migration.

Further support is obtained by methods that probe the existence and properties of the salt film. Electrochemical impedance spectroscopy (EIS) is one method that has proven useful, although in theory other non-steady-state electrochemical methods can provide similar or the same information.

Once a salt film precipitates on the electrode surface, the film is not likely to be stagnant. Rather, the film continually precipitates and dissolves; at steady state, however, the dissolution rate must equal the precipitation rate, leading to a time-invariant film thickness. The details of the film growth and dissolution mechanism are not discussed here, but may be important, as indicated in the next section.

The steady-state film thickness depends not only on the mixing conditions of the process but also on the applied electrode potential. From a theoretical perspective, the film thickness increases with potential until the total resistance of the system is such that the surface overpotential (driving the metal oxidation rate) is a value that enables the film growth and dissolution rates to be equal. The film dissolution rate is controlled by mass transfer through the diffusion layer. Stated another way,

keeping the dissolution rate of the film constant, an increase in applied potential results in film thickening until the electrical-potential drop across the film equals the change in total applied potential. The manner in which the film thickness varies with the applied potential depends on the nature of the transport processes and the properties of the film itself.

Transient electrochemical methods, such as EIS, provide a direct measure of the film resistance. A major drawback to analysis via EIS is that, while the analysis is readily performed, interpretation can be difficult, especially for the uninitiated. In addition to providing a measure of the film resistance, the spectra obtained provide information about whether the film resistances are in series or in parallel with a capacitive component of the process, whether the system capacitance is associated with charging of the electrolyte double layer or with charging of the film itself. When using EIS to test a salt-film-mechanism hypothesis, the high-frequency range of the spectrum may be particularly valuable. A physical interpretation of the low-frequency part of the spectra has sometimes been more elusive.

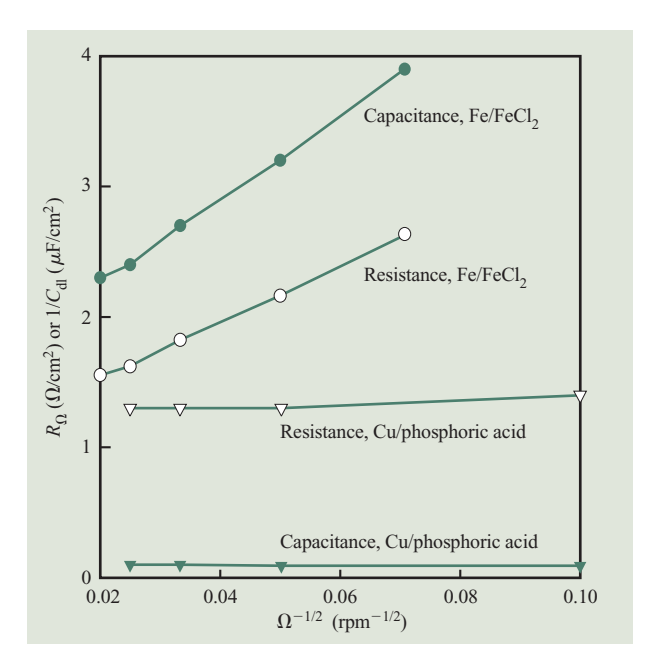
Focusing on the high-frequency range, *any* of the following may suggest the formation of a salt film:

- The ohmic resistance (high-frequency limit of the EIS) changes with applied potential or rotation speed and is significantly larger than the electrolyte resistance.
- 2. The electrode capacitance changes with applied potential or rotation speed and is significantly smaller than the capacitance of the expected value for a bare electrode of  $10-100 \ \mu F/cm^2$ .
- 3. The polarization resistance changes with applied potential within the limiting-current plateau (for a given electrode rotation speed).

Measured changes should also be expected to show systematic variations with rotation speed (assuming the use of a rotating disk electrode) and applied potential. For example, **Figure 4** shows the variation with rotation speed of the high-frequency limit of the EIS,  $R_{\Omega}$ , and the reciprocal of the apparent double-layer capacitance,  $C_{\rm dl}$ , of the Fe/FeCl<sub>2</sub> electropolishing system [43]. Interestingly, the order of magnitude of the double-layer capacitance is 0.1–1.0  $\mu$ F/cm<sup>2</sup>, which is much lower than expectations for a bare electrode. Both  $R_{\Omega}$  and  $C_{\rm dl}$  vary linearly with  $\Omega^{-1/2}$ , which is proportional to the diffusion-layer thickness. These variables also display a nearly linear dependence on the applied potential.

The manner in which the measurements vary with the operating conditions plays a key role in the development of a detailed model describing the mechanisms of film growth and dissolution as well as the transport processes





Measured ohmic resistance and apparent double-layer capacitance as a function of the (rotation speed) $^{-1/2}$  for iron dissolution at the limiting current density in an FeCl $_2$  electrolyte [43] and copper dissolution into 85-wt.% phosphoric acid [25]. The iron electropolishing process shows systematic variations in these properties as a function of operating conditions, implying that a salt-film mechanism is applicable.

within the film. Frequently, it is found that the film growth and transport processes cannot be modeled simply, and duplex-film structures are invoked [43, 48–51]. The apparently complex nature of the films prevents the use of an EIS analysis to estimate film thickness; this may be a practical consideration, as discussed in the next section. *In situ* optical methods may be useful, although these may also require a model of the film structure to obtain an unambiguous thickness [52]. Flow modulation spectroscopy also appears to provide information that is complementary to EIS, and may enable film-thickness estimation [53].

Figure 4 shows comparative results for iron dissolution in an FeCl<sub>2</sub> electrolyte and for copper electropolishing in 85-wt.% phosphoric acid [25]. For the Cu/phosphoric-acid system, both the high-frequency resistance and the double-layer capacitance are independent of rotation speed and applied potential (not shown here). Furthermore,  $C_{\rm dl}$  was measured to be approximately  $10~\mu{\rm F/cm}^2$ , and the polarization resistance at a given rotation speed was not a function of potential on the limiting-current plateau. These results support the idea that an acceptor mechanism, discussed below, is applicable for this system.

## Acceptor mechanism

While convincing experimental evidence can be obtained in some instances to support salt-film mechanisms, the experimental evidence in support of acceptor mechanisms is more subtle, frequently being the lack of data that support a salt-film mechanism.

For the Cu/phosphoric-acid electropolishing system, an acceptor mechanism appears to be applicable [25]. A simple mechanism can be written as

$$Cu \rightarrow Cu_{ads}^{2+} + 2e^{-}, \tag{10}$$

$$s_{\rm A}A + {\rm Cu}_{\rm ads}^{2+} \rightarrow {\rm Cu}^{2+} \cdot {\rm A}_{sA}({\rm aq}),$$
 (11)

with the process being limited by diffusion of the acceptor A to the electrode surface. For this example, the limiting current density on a rotating disk electrode can be written as

$$i_{\text{lim}} = 0.62 n F \Omega^{1/2} \left( D_{\text{A}}^{2/3} v^{-1/6} \frac{c_{\text{A},\infty}}{s_{\text{A}}} \right),$$
 (12)

where all of the terms in the parentheses on the righthand side of the equation are perhaps unknown, although the kinematic viscosity v can be independently measured.

Studies of the influence of electrolyte composition on copper electrodissolution rates in phosphoric-acid electrolytes cannot be unambiguously interpreted. The addition of a cupric salt to the electrolyte causes a decline in the limiting-current density, qualitatively consistent with a salt-film mechanism. Nevertheless, much of the decrease in current density can be explained by changes in the transport properties of the electrolyte [54]. The addition of water to the electrolyte causes an increase in the current density, consistent with a water acceptor mechanism. Nevertheless, the addition of water also affects the transport properties in a manner that could account for at least some of the increase in current density.

EIS has been used to investigate the Cu/phosphoricacid system, leading to support for an acceptor mechanism. Specifically, the measured EIS spectra do not show any of the signatures highlighted above, suggesting that there is no salt film present. Furthermore, the application of flow modulation spectroscopy provides a measure of the diffusion time constant, allowing for the determination of the diffusion coefficient  $D_{\Lambda}$  [cf. Equation (12)] of the acceptor independent of knowledge of its bulk concentration [55]. A limiting-current measurement alone permits only determination of the product of the diffusion coefficient and (unknown) acceptor concentration. Once  $D_{\rm A}$  is known from the flow modulation spectra, Equation (12) can be applied to limiting-current density measurements to obtain  $(c_{A,\infty}/s_A)$ , which was found to be 2.3 M at temperatures

of 36°C and 93°C. In a salt-film mechanism, the relevant concentration is the saturation concentration of the salt, which would not be expected to be independent of temperature.

Assuming  $s_{\rm A}=6$ , the expected number of water molecules that complex cupric ions, the bulk concentration was found to be 14 M; in comparison, the molar concentration of water in 85-wt.% phosphoric acid is 13.6 M. It was concluded then that water is the acceptor molecule, consistent with previous conclusions [56] and in contrast to earlier work [57] that hypothesized an anionic acceptor.

# **Electrochemical planarization**

The planarization of a surface containing topological features can be achieved via a process sometimes known as anodic leveling. Anodic leveling phenomena are more easily understood than those associated with cathodic leveling, where the precise mechanism associated with the organic leveling agents is not always clear. In short, a theoretical or numerical simulation, assuming a masstransfer-controlled dissolution rate, can be performed [58, 59]. The rate of dissolution on the planar surface outside the feature is higher than the rate at the bottom, as depicted in Figure 5. Similar concepts have also been applied to cathodic leveling, except that nonlinearities between the deposition rate and the flux of organic additives to a surface may lead to more rapid leveling than may be commonly attainable during anodic leveling [60].

The difference between  $u_2$  and  $u_1$  in Figure 5 is important in predicting leveling efficacy. This difference depends on the ratio of the feature size to the diffusion layer thickness, as well as the aspect ratio of the feature. The ratio of course also evolves in time. For example, if the etching process is nearly isotropic, the feature should be expected to open up rapidly, significantly decreasing the aspect ratio and thus the difference in the interfacial velocities. If the mechanism is well understood, the interfacial velocity can be readily tracked as a function of space and time with standard simulation tools, such as EVOLVE, that allow for tracking of the interface [61].

The value of the interfacial-velocity difference may or may not be easy to predict, depending on the reaction mechanism and on the hydrodynamics of the process. For example, when features are relatively large compared with the hydrodynamic boundary layer that would exist near a planar surface, the feature may affect the flow, causing the boundary layer to follow the contour of the feature. In such cases, prediction of the spatial variation in the current distribution requires computational fluid dynamics to first determine fluid flow perhaps throughout the entire electrochemical cell before the mass transfer can be resolved. Assuming the flow generated by a

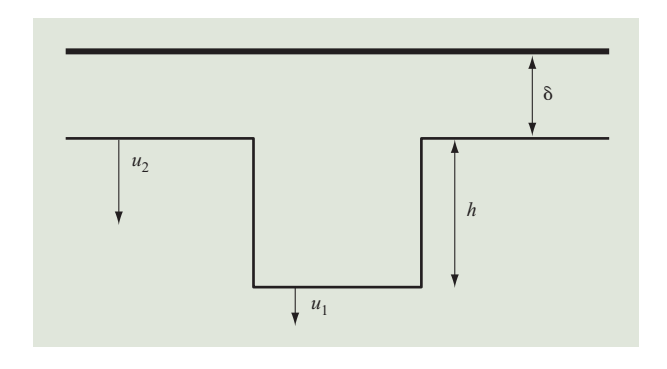


# Figure 5

Schematic diagram of a feature of height h to be planarized. For simplicity, the diffusion layer is assumed to be of uniform thickness  $\delta$ . Since the diffusion path from the exterior surface to the bulk is shorter than that from the feature bottom to the bulk, the dissolution rate  $u_2$  is greater than  $u_1$ , leading to planarization.

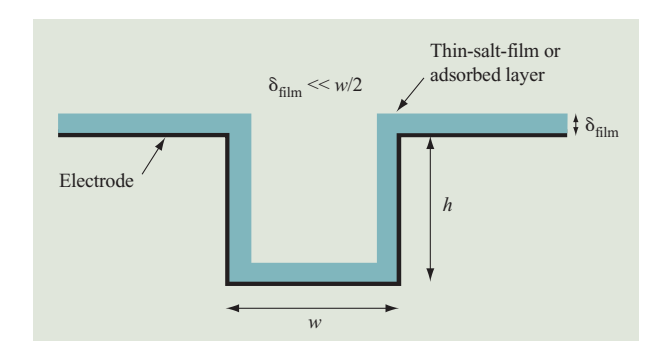
rotating disk electrode, the momentum boundary layer thickness is given by

$$\delta_{\text{mom}} = 1.61 \Omega^{-1/2} v^{-1/2}. \tag{13}$$

For a rotation speed  $\Omega=100$  rpm  $(10.5~{\rm s}^{-1})$  and a relatively large kinematic viscosity  $v=0.3~{\rm cm}^2/{\rm s}$  for a phosphoric-acid type electrolyte,  $\delta_{\rm mom}$  is calculated to be 2.7 mm, which is significantly larger than a typical feature.

In the second extreme, the feature is small compared with the boundary layer, and the mass-transfer phenomena can be adequately analyzed by the so-called stagnant diffusion-layer model, in which the boundary layer is assumed not to be perturbed by the feature, and convection within the layer is neglected. For this model, it is sufficient to characterize the flow and external mass transfer with a diffusion-layer thickness  $\delta$ . The model is easily treated with simulation tools and is frequently useful in process design considerations, especially for feature sizes of the order of a few  $\mu$ m or less.

The reaction mechanism may also significantly influence the efficacy and complexity of electrochemical-planarization simulation tools. **Figure 6** shows an example of this, assuming that an acceptor mechanism applies. In an acceptor mechanism, the reaction rate is limited by the transport of a species that accepts the adsorbed, oxidized species from the electrode surface. Since the adsorbed layer is confined very near the electrode surface, implementation of an acceptor mechanism into a two- or three-dimensional simulation tool is straightforward, at least for a feature-scale simulation that is uncoupled from the wafer-scale problem.



Schematic diagram illustrating an electrode with feature height h and width w undergoing dissolution. It is assumed that either an acceptor mechanism or a thin-salt-film mechanism applies. When the film thickness  $\delta_{\text{film}}$  is much smaller than w/2, the film follows the substrate, and the current and reaction product flux through the film is everywhere perpendicular to the electrode surface, greatly facilitating the development of a mathematical description of the planarization process.

The implementation of the salt-film mechanism in such a simulation tool may be straightforward, depending on the salt-film thickness. For example, when the film thickness is small compared with feature size, the film follows the contours of the substrate. The transport processes within the film need not be described in detail, because transport proceeds in only one dimension normal to the metal surface. Simulation tool development thus remains straightforward, and the anodic leveling behavior of this "thin-salt-film" system should be essentially the same as that of an acceptor system.

Interfacial velocities can be effectively estimated from Equation (1). The current density, which is assumed to be mass-transfer-limited, is proportional to the normal flux to the surface of the rate-limiting species (either an acceptor to the surface or cupric ions away from the salt film). The current distribution, assuming steady-state operation, can thus be estimated from Laplace's equation

$$\nabla^2 c = 0, (14)$$

subject to the following boundary conditions: at  $y=\delta$ ,  $c=c_\infty$ ; at the electrode surface,  $c=c_0$ , where the surface concentration  $c_0$  is zero for an acceptor theory and  $c_{\rm sat}$  for a salt film. The numerical solution to this problem depends only on the aspect ratio of the feature and the ratio of the feature height h to the diffusion-layer thickness  $\delta$ .

Assuming again a rotating disk electrode, the diffusion layer thickness  $\delta = \delta_{\text{mom}}(v^{-1/3}/D)$ . For a phosphoric acid electrolyte, the ratio of kinematic viscosity to diffusion coefficient  $(v/D) \approx 10^6$  at 35°C, implying that  $\delta \approx 27 \, \mu\text{m}$ ,

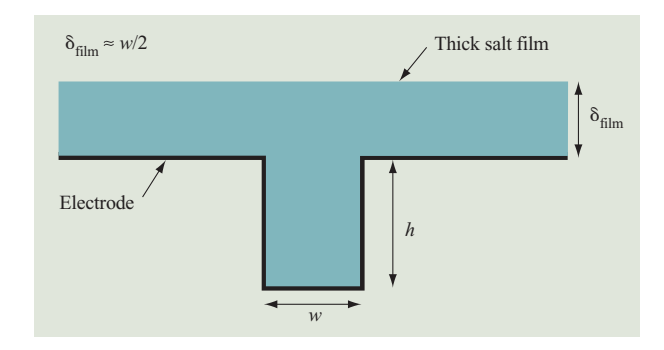


## Figure 7

Schematic diagram illustrating an electrode with feature height h and width w undergoing dissolution. It is assumed that the film thickness  $\delta_{\rm film}$  on the exterior surface is larger than the feature half width w/2, implying that the salt film completely fills the feature. Calculation of the redistribution of the current from the electrolyte/film interface to the film/electrode interface (and even the precise shape of the electrolyte/film interface) requires an understanding of the film growth and transport properties.

given that  $\delta_{\text{mom}} = 2.7$  mm. The ratio  $h/\delta$  is thus typically very small.

The assumption of mass-transfer-controlled dissolution in this feature-scale model may not be satisfied over the entire surface of a wafer, as discussed in the Introduction. Even if the assumption is satisfied, the influence of electrical migration may also affect the magnitude of the dissolution rate. However, on the feature scale, electrical migration is *not* likely to lead to a significant change in the distribution of the current density when normalized by the spatial average current density [62, 63].

Instead, assume that the electrolyte and operating conditions are chosen so that the film is sufficiently thick that the entire feature is filled with salt, as shown in **Figure 7**. In this case, the film shape and thickness above the feature are not known *a priori* but must be determined. For the case of a steady-state process, the film shape is calculated to satisfy the requirement that the rate of film creation must be equal to the rate of film dissolution. The film-thickness constraint is also true for a thin film; however, the film thickness as a function of position on the substrate need not be calculated to perform the type of planarization simulation outlined above, because such a film is too thin for the current to redistribute from the electrolyte/film interface to the metal/film interface.

However, once the film thickness is of the order of magnitude of the size of the underlying features, the current distribution within the salt film must be determined and depends on the physical properties of the film. It is thus difficult to predict the evolution of the interface shape without a detailed understanding

of associated film-transport mechanisms. This understanding of the film transport processes is often somewhat limited [43, 48–51, 53] and can lead to quite different estimates of the salt-film thickness [64]. For example, West et al. conclude that, for the dissolution of iron in ferrous chloride electrolytes, the film thickness can range from 0.1 to 1.0  $\mu$ m at low rotation speeds, depending on the modeling details [53]. Since the larger thicknesses are of the order of magnitude of anticipated feature sizes relevant to planarization technologies, the "thick"-film planarization scenario may become relevant.

# **Summary**

The electropolishing of copper from phosphoric acid has been known for many decades, and now shows promise for the planarization of on-chip interconnect metallization. Both salt-film and acceptor mechanisms, which can sometimes be indirectly confirmed with electrochemical methods, have been invoked to explain the mass-transfer-limited dissolution rates that are required to achieve the electropolishing of on-chip interconnect metallization. Mass-transfer-controlled electrodissolution can be simulated straightforwardly when an acceptor or a thin-salt-film mechanism applies. In contrast, when the film thickness is of the order of the size of the substrate features, predictions may be more difficult, requiring detailed knowledge of the associated film-transport processes.

# Appendix: List of symbols

- c concentration, mol/cm<sup>3</sup> or mol/1
- $C_{\rm dl}$  double layer capacitance,  $\mu F/\text{cm}^2$
- D diffusion coefficient, cm<sup>2</sup>/s
- F Faraday's constant, 96,487 coulombs/mole
- h feature height, cm
- *i* current density, A/cm<sup>2</sup>
- $K_{\rm sp}$  solubility product,  $M^3$
- n number of electrons transferred
- $r_0$  wafer or disk radius, cm
- $R_{\Omega}$  high-frequency resistance,  $\Omega/\text{cm}^2$
- s<sub>A</sub> stoichiometric coefficient
- u etch rate, cm/s
- $V_{\rm m}$  molar volume of copper metal, cm<sup>3</sup>/mol
- w feature width, cm
- $\delta$  mass-transfer boundary layer thickness, cm
- $\delta_{\rm mom}$  momentum boundary layer thickness, cm
- $\delta_{\rm film}~$  salt film thickness, cm
- $\kappa$  electrolyte conductivity,  $\Omega^{-1}$ -cm<sup>-1</sup>
- v kinematic viscosity, cm<sup>2</sup>/s
- $\phi$  potential of substrate or electrolyte, V
- $\sigma$  substrate conductivity,  $\Omega^{-1}$ -cm
- λ substrate thickness, cm
- $\Omega$  disk or wafer rotation speed, rpm or s<sup>-1</sup>

# Subscripts

A acceptor

Cl chloride ions

Fe ferrous ions

FeCl, ferrous chloride

lim limiting

0 surface

sat saturated

∞ bulk

# **Acknowledgments**

Many thanks to John Cotte for helpful discussions and to Min Zheng for help with the figures.

### References

- A. C. West, S. Mayer, and J. Reid, *Electrochem. & Solid State Lett.* 4, C50 (2001).
- T. P. Moffat, D. Wheeler, W. H. Huber, and D. Josell, Electrochem. & Solid-State Lett. 4, C26 (2001).
- J. W. Dini, "Electrodeposition of Copper," in Modern Electroplating, Fourth edition, M. Schlesinger and M. Paunovic, Eds., John Wiley & Sons, New York, 2000.
- B. M. Basol, C. E. Uzoh, H. Talieh, D. Young, P. Lindquist, T. Wang, and M. Cornejo, *Microelectron. Eng.* 64, 43 (2002).
- J. M. Steigerwald, S. P. Murarka, and R. J. Gutmann, Chemical Mechanical Planarization of Microelectronic Materials, Wiley, New York, 1997.
- C. L. Borst, D. G. Thakurta, W. N. Gill, and R. J. Gutman, J. Electron. Packag. 124, 262 (2002).
- X. Xiao, N. Hata, K. Yamada, and T. Kikkawa, Rev. Sci. Instrum. 74, 4539 (2003).
- 8. J. Huo, R. Solanki, and J. McAndrew, Surf. Eng. 19, 11 (2003).
- R. Contolini, A. F. Bernhardt, and S. T. Mayer, J. Electrochem. Soc. 141, 2503 (1994).
- S. Mayer, R. Contolini, and A. Bernhardt, U.S. Patent 5,095,550, 1992.
- R. J. Contolini, S. T. Mayer, R. T. Graff, L. Tarte, and A. F. Bernhardt, Solid State Technol. 40, 155 (1997).
- 12. D. Padhi, J. Yahalom, S. Gandikota, and G. Dixit, *J. Electrochem. Soc.* **150**, G10 (2003).
- S.-H. Chang, J.-M. Shieh, B.-T. Dai, M.-S. Feng, Y.-H. Li,
  C. H. Shih, H. M. Tsai, S. L. Shue, R. S. Liang, and
  Y.-L. Wang, Electrochem. & Solid-State Lett. 6, G72 (2003).
- S.-H. Chang, J.-M. Shieh, C.-C. Huang, B.-T. Dai, and M.-S. Feng, *Jpn. J. Appl. Phys.* 41, 7332 (2002).
- S.-H. Chang, J.-M. Shieh, C.-C. Huang, B.-T. Dai, and M.-S. Feng, J. Vac. Sci. Technol. B 20, 2149 (2002).
- J. Huo, R. Solanki, and J. McAndrew, J. Appl. Electrochem. 34, 305 (2004).
- 17. M. Datta, J. Electrochem. Soc. 142, 3801 (1995).
- E. Rosset, M. Datta, and D. Landolt, *Plating & Surf. Finish.* 72, 60 (1985).
- D. Landolt, R. H. Muller, and C. W. Tobias, *J. Electrochem. Soc.* 118, 36 (1971).
- 20. M. Datta and D. Landolt, Electrochim. Acta 25, 1263 (1979).
- R. Rosenberg, D. C. Edelstein, C.-K. Hu, and K. P. Rodbell, *Ann. Rev. Mater. Sci.* 30, 229 (2000).
- 22. M. E. Gross, C. Lingk, W. L. Brown, and R. Drese, *Solid State Technol.* 42, 47 (1999).
- N. Ibl, in Advances in Electrochemistry and Electrochemical Engineering, P. Delahay and C. W. Tobias, Eds., John Wiley, New York, 1962, p. 49.
- D. P. Barkey, R. H. Muller, and C. W. Tobias, *J. Electrochem. Soc.* 136, 2199 (1989).

- R. Vidal and A. C. West, J. Electrochem. Soc. 142, 2682 (1995).
- J. S. Newman, *Electrochemical Systems*, Second edition, Prentice-Hall, Inc., Englewood Cliffs, NJ, 1991, p. 388.
- C. W. Tobias and R. Wijsman, J. Electrochem. Soc. 100, 459 (1953).
- 28. M. Matlosz, P.-H. Vallotton, A. C. West, and D. Landolt, J. Electrochem. Soc. 139, 752 (1992).
- 29. K. Takahashi, J. Electrochem. Soc. 147, 1414 (2000).
- W. E. Corbin, Jr., M. Datta, T. E. Dinan, and F. W. Kern, U.S. Patent 5,865,984, 1999.
- 31. P. A. Jacquet, Nature 135, 1076 (1935).
- 32. T. P. Hoar and J. A. Mowat, Nature 165, 64 (1950).
- W. J. McTegart, The Electrolytic and Chemical Polishing of Metals, Pergamon Press, London, 1956.
- 34. D. Landolt, Electrochim. Acta 32, 1 (1987).
- D. Landolt, "Mass Transport Processes in High Rate Metal Dissolution and Deposition," *Proceedings of the Symposium* on High-Rate Metal Dissolution Processes, M. Datta, B. R. MacDougall, and J. M. Fenton, Eds., The Electrochemical Society, Pennington, NJ, 1995, pp. 1–15.
- 36. M. Datta, IBM J. Res. & Dev. 42, 655 (1998).
- 37. J. S. Newman, *Electrochemical Systems*, Second edition, Prentice-Hall, Inc., Englewood Cliffs, NJ, 1991, pp. 341–345.
- 38. G. Prentice, *Electrochemical Engineering Principles*, Prentice-Hall, Inc., Englewood Cliffs, NJ, 1991.
- A. J. Bard and L. R. Faulkner, Electrochemical Methods. Fundamentals and Applications, Second edition, John Wiley & Sons, New York, 2001.
- 40. R. Vidal and A. C. West, J. Electrochem. Soc. 145, 4067 (1998).
- 41. R. Vidal and A. C. West, Electrochim. Acta 41, 2417 (1996).
- 42. M. Novak, A. K. N. Reddy, and H. Wroblowa, *J. Electrochem. Soc.* 117, 733 (1970).
- R.-D. Grimm, A. C. West, and D. Landolt, *J. Electrochem. Soc.* 139, 1622 (1992).
- T. P. Hoar, D. C. Mears, and G. P. Rothwell, *Corrosion Sci.* 5, 279 (1965).
- 45. M. Datta and D. Landolt, Electrochim. Acta 25, 1255 (1980).
- 46. H. C. Kuo and D. Landolt, *Electrochim. Acta* 20, 393 (1975).
- J. S. Newman, *Electrochemical Systems*, Second edition, Prentice-Hall, Inc., Englewood Cliffs, NJ, 1991, pp. 397–425.
- 48. H.-H. Strehblow and J. Wenners, *Electrochim. Acta* 22, 421 (1977).
- 49. C. Clerc and D. Landolt, Electrochim. Acta 33, 859 (1988).
- 50. T. R. Beck, Electrochim. Acta 30, 725 (1985).
- 51. C. Clerc and R. Alkire, J. Electrochem. Soc. 138, 25 (1991).
- R. M. A. Azzam and N. M. Bashara, Ellipsometry and Polarized Light, Elsevier Science Publishers, Amsterdam, 1987
- 53. A. C. West, R.-D. Grimm, D. Landolt, C. Deslouis, and B. Tribollet, *J. Electroanalyt. Chem.* **330**, 693 (1992).
- 54. D. T. Chin and H. Chang, J. Appl. Electrochem. 19, 95 (1989).
- R. Vidal and A. C. West, J. Electrochem. Soc. 142, 2689 (1995).
- S. H. Glarum and J. H. Marshall, J. Electrochem. Soc. 132, 2872 (1985).
- 57. J. Edwards, J. Electrochem. Soc. 100, 189C (1953).
- 58. C. Wagner, J. Electrochem. Soc. 101, 225 (1954).
- M. Matlosz and D. Landolt, J. Electrochem. Soc. 136, 919 (1989).
- R. Chalupa, Y. Cao, and A. C. West, J. Appl. Electrochem. 32, 135 (2002).
- 61. Y. H. Im, M. O. Bloomfield, S. Sen, and T. S. Cale, *Electrochem. & Solid-State Lett.* **6**, C42 (2003).
- 62. J. D. Yang and A. C. West, AIChE J. 43, 811 (1997).
- 63. D. R. Baker, M. W. Verbrugge, and J. Newman, J. Electroanal. Chem. 313, 23 (1991).
- 64. A. C. West, J. Electrochem. Soc. 140, 403 (1993).

Received January 12, 2004; accepted for publication June 1, 2004; Internet publication December 7, 2004

Alan C. West Department of Chemical Engineering, Columbia University, New York, New York 10027 (acw17@columbia.edu). Dr. West is Professor of Chemical Engineering at Columbia University. He received a B.S. degree in chemical engineering in 1985 from Case Western Reserve University and a Ph.D. degree in 1989 from the University of California at Berkeley, also in chemical engineering. This paper was written during 2003 and 2004 while he was an Academic Visitor at the IBM Thomas J. Watson Research Center in Yorktown Heights, New York. His research interests are motivated by the design of electrochemical processes and devices.

Hariklia Deligianni IBM Research Division, Thomas J. Watson Research Center, P.O. Box 218, Yorktown Heights, New York 10598 (lili@us.ibm.com). Dr. Deligianni manages the Electrochemical Processes Group at the Thomas J. Watson Research Center. She received a B.S. degree in chemical engineering from Aristotelion University, Thessaloniki, Greece, in 1982, and M.S. and Ph.D. degrees from the University of Illinois at Urbana-Champaign in 1986 and 1988, respectively. Since joining IBM in 1988, she has successfully introduced electrochemical processes into the solder-based C4 technology, playing a key role in developing the processes and transferring them to IBM manufacturing. As well as being a key participant in the study of the feasibility of copper metallization for on-chip interconnects, she later developed mathematical models for the design and operation of electrodeposition tools and process models of feature filling during copper electroplating for such interconnects. Throughout her 16 years at IBM, Dr. Deligianni has worked on diverse and interesting projects such as the integration of passives and MEMS for wireless communications. More recently, her group has been working to develop electrochemical processes for fabrication of future CMOS logic chips. Dr. Deligianni has received an IBM Corporate Technical Excellence Award, an IBM Outstanding Innovation Award, and IBM Patent Awards. She holds ten patents and is an author of 40 publications in technical journals and conference proceedings. Dr. Deligianni is a member of the Executive Committee of the Electrodeposition Division of the Electrochemical Society, a member of the Electrochemical Society, a member of the American Institute of Chemical Engineers, and a member of IEEE.

Panayotis C. Andricacos IBM Research Division, Thomas J. Watson Research Center, P.O. Box 218, Yorktown Heights, New York 10598 (ndricac@us.ibm.com). Dr. Andricacos, who passed away on November 21, 2004, was a manager in the Silicon Science and Process Technology Department at the IBM Thomas J. Watson Research Center. He received B.S., M.S., and doctoral degrees in chemical engineering from Columbia University, where he was also an adjunct associate professor. As a postdoctoral research associate at the Lawrence Berkeley Laboratories, he worked on fuel cells and on the application of ultrahigh-vacuum techniques to the study of electrochemical reactions. While at IBM, Dr. Andricacos worked on the application of electrochemical processes in storage, packaging, and C4 technologies; he played a pioneering role in the development of copper electroplating for semiconductor on-chip metallization. In 1993, he received the Research Award of the Electrodeposition Division, Electrochemical Society, for the development of novel techniques for the study of alloy electroplating.